Luminescence Properties and Crystal Structures of Dicyano(diimine)platinum(II) Complexes Controlled by Pt···Pt and $\pi-\pi$ Interactions

Masako Kato,*[,1a] Chizuko Kosuge,[1a] Katsuyuki Morii,[1b] Jeung Sun Ahn,[1b] Hiroshi Kitagawa,[1b] Tadaoki Mitani,[1b] Michio Matsushita,[1c] Tatsuhisa Kato,[1c] Shigenobu Yano,[1a] and Masaru Kimura[1a]

Department of Chemistry, Faculty of Science, Nara Women's University, Nara 630-8506, Japan, Institute for Molecular Science, Okazaki 444-8585, Japan, and Japan Advanced Institute of Science and Technology, Hokuriku, Tatsunokuchi, 923-1292, Japan

Received August 25, 1998

Introduction

Platinum(II) complexes with α-diimines often display characteristic color and emission in the solid state on the basis of the Pt−Pt interaction.[2] The red form of $[Pt(CN)_2(bpy)]$ (bpy = 2,2′-bipyridine) is known as one of typical examples. It has a stacking structure of the $[Pt(CN)_2(bpy)]$ units with a Pt···Pt distance of 3.35 Å at room temperature.[3] The crystal exhibits intense red emission around 600 nm even at room temperature, which is not observed for the monomeric form in dilute solution.[4] The emission is assigned to that from the metal-to-ligand charge transfer state, ^{3}MLCT [dσ*(Pt)→π*(bpy)], where dσ*(Pt) occurs from the Pt···Pt electronic interactions. Gliemann et al. reported that the emission maximum is shifted to longer wavelength with lowering temperature.[5] Such striking temperature dependence of the emission spectrum have been noted for several linear-chain platinum complexes such as $M_x[Pt(CN)_4]\cdot nH_2O$[6] and $[PtCl_2(bpy)]$,[2] and ascribed to the change of the Pt···Pt intermolecular interactions. The shrinkage of the Pt···Pt distance with lowering temperature has been observed as the direct evidence.[6,7] Thus the variable-temperature data of the Pt···Pt distance corresponding to the emission data are definitely needed also for the $[Pt(CN)_2(bpy)]$ complex.

As another linear-chain platinum complex, we have recently synthesized and characterized dicyano(3,3′-biisoquinoline)platinum(II) including an extended π-system, $[Pt(CN)_2(i\text{-biq})]\cdot 0.5H_2O$.[8] The Pt···Pt distance (3.34 Å) and the emission maximum (λ_{max} = 610 nm) are very similar to those of the corresponding bpy complex at room temperature. At 77 K, however, the quite different luminescence spectral feature was observed.

Table 1. Crystallographic Data for $[PtCN_2(i\text{-biq})]\cdot 0.5H_2O$

formula: $PtN_4C_{20}H_{13}O_{0.5}$	fw = 512.44
cryst system: orthorhombic	space group: *Pbca* (no. 61)
a = 27.99(1) Å	T = 293 K
b = 18.318(8) Å	λ = 0.71073 Å
c = 6.68(1) Å	ρ_{calc} = 1.987 g cm^{-3}, ρ_{obs} = 1.99 g cm^{-3}
V = 3425(8) Å^3	μ(Mo Kα) = 8.172 mm^{-1}
Z = 8	$R_1{}^a$ = 0.040
	$wR_2{}^b$ = 0.143

[a] $R_1 = \sum||F_o| - |F_c||/\sum|F_o|$. [b] $wR_2 = [\sum w(F_o^2 - F_c^2)^2/\sum w(F_o^2)^2]^{1/2}$, $w = [\sigma_c^2(F_o^2) + (0.0030F_o^2)^2]^{-1}$.

In this work, we have accomplished the study of the temperature dependence of both emission spectrum and crystal structure of $[Pt(CN)_2(i\text{-biq})]\cdot 0.5H_2O$ as well as $[Pt(CN)_2(bpy)]$. We report a good correlation of the emission spectrum and the Pt···Pt distance for $[Pt(CN)_2(bpy)]$ and unique behavior of the $[Pt(CN)_2(i\text{-biq})]\cdot 0.5H_2O$ crystal. The revised crystal structure of $[Pt(CN)_2(i\text{-biq})]\cdot 0.5H_2O$ are also reported here which is proved by careful reinvestigation to have the unit cell with the double of the *a* axis reported previously.[8]

Experimental Section

Materials. The red form of $[Pt(CN)_2(bpy)]$ was prepared according to the literature procedure.[4] The preparation of $[Pt(CN)_2(i\text{-biq})]$ was reported previously.[8]

X-ray Crystallography. The X-ray diffraction data of the red form of $[Pt(CN)_2(bpy)]$ were obtained at the temperature range from 318 to 10 K on a Rigaku AFC-7R four-circle diffractometer and a MAC Science imaging-plate system with graphite monochromated Mo Kα radiation using the closed-cycle cryostat. Because of the lowering quality of single crystals, the variable temperature measurements were accomplished by replacing crystals several times. The crystal data at room temperature were consistent with those reported by Connick et al.[3] The space group of *Cmcm* was kept during the temperature range measured. The crystal structures were determined by the direct method.[9a] The structures were refined with anisotropic temperature factors for the non-H atoms. The final R_1 values were about 0.04 for the structures at any temperatures.

The data for an orange-red plate crystal of $[Pt(CN)_2(i\text{-biq})]\cdot 0.5H_2O$ were collected on a Rigaku AFC-7R equipped with a liquid nitrogen cryostat. The crystal lattice was determined every 15 K from 293 to 210 K. The diffraction data at 293 and 220 K were collected using $\omega-2\theta$ scan technique to a maximum 2θ value of 55°. Pertinent crystallographic data at 293 K are summarized in Table 1. The structure was solved by heavy-atom Patterson methods[9b] and expanded using Fourier techniques.[10] For the data at 293 K, the non-hydrogen atoms except the oxygen atom for crystal water were refined anisotropically. In the present unit cell, the positions of all atoms were reasonably determined though there were the disorder problems in the previous analysis.[8] Calculations of full matrix least-square refinement under the situation converged nicely with normal bond lengths and angles. The hydrogen atoms were included but not refined. The final cycle of full-matrix least-squares refinement was based on 3950 observed reflections ($I > 0.00\sigma(I)$) and 230 variable parameters. The final R indices are listed in Table 1. As for the analysis at 220 K, only the platinum atom was refined anisotropically, while the rest were refined isotropically because of the low quality of the data. However, the structure was

(1) (a) Nara Women's University. (b) Japan Advanced Institute of Science and Technology. (c) Institute for Molecular Science.
(2) Houlding, V. H.; Miskowski, V. M. *Coord. Chem. Rev.* **1991**, *111*, 145−152.
(3) Connick, W. B.; Henling, L. M.; Marsh, R. E. *Acta Crystallogr.* **1996**, *B52*, 817−822.
(4) Che, C.-M.; He, L.-Y.; Poon, C.-K.; Mak, T. C. W. *Inorg. Chem.* **1989**, *28*, 3081−3083.
(5) Biedermann, J.; Wallfahrer, M.; Gliemann, G. *J. Lumin.* **1987**, *37*, 323−329.
(6) Gliemann, G.; Yersin, H. *Struct. Bonding* **1985**, *62*, 87−153.
(7) Connick, W. B.; Henling, L. M.; Marsh, R. E.; Gray, H. B. *Inorg. Chem.* **1996**, *35*, 6261−6265.
(8) Kato, M.; Sasano, K.; Kosuge, C.; Yamazaki, M.; Yano, S.; Kimura, M. *Inorg. Chem.* **1996**, *35*, 116−123.
(9) (a) SIR92: Altomare, A., Burla, M. C., Camalli, M., Cascarano, M., Giacovazzo, C., Guagliardi, A., Polidori, G., *J. Appl. Crystallogr.* **1994**, *27*, 435. (b) PATTY: Beurskens, P. T., Adamirral, G., Beurskens, G. Bosman, W. P., Garcia-Granda, S., Gould, R. O., Smits, J. M. M.; Smykalla, C., 1992.
(10) The DIRDIF program system, Technical Report of the Crystallography Laboratory, University Nijmegen, The Netherlands, 1994.

10.1021/ic981027a CCC: $18.00
Published on Web 03/13/1999

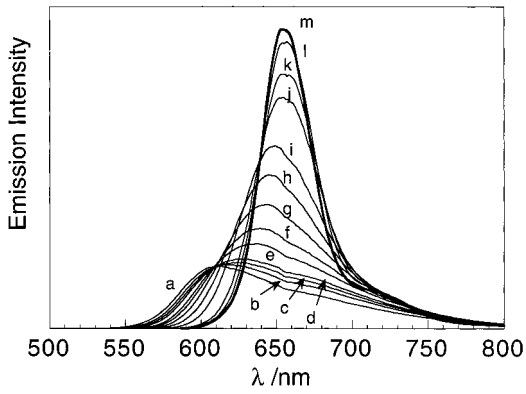

Figure 1. Emission spectra of the red form of $[Pt(CN)_2(bpy)]$ at different temperatures: (a) 292, (b) 260, (c) 240, (d) 220, (e) 180, (f) 160, (g) 140, (h)120, (i) 100, (j) 60, (k) 45, (l) 30, (m) 15 K. λ_{ex} = 514.5 nm.

converged with a slightly large value of R_1 (0.077), and the results gave important information about the packing structure (vide infra). Crystal data, experimental details, and positional and thermal parameters for all crystals are included in the Supporting Information. All calculations were performed using the teXsan crystallographic software package.[11]

Emission Spectroscopy. The variable-temperature emission measurement for the $[Pt(CN)_2(bpy)]$ crystal was performed using a continuous-flow cryostat (Oxford Optistat^{CF}) with excitation at 514.5 nm by an argon ion laser. A red-sensitivity-enhanced photomultiplier (Hamamatsu R5509−41, cooled to 203 K) was used as a detector. The excitation intensity employed in this experiment was so low that the luminescence intensity varied with it linearly. Emission spectra of the $[Pt(CN)_2(i\text{-biq})]\cdot 0.5H_2O$ crystal were obtained on a Hitachi 850 spectrofluorimeter and a Nikon P-250 spectrometer with a photomultiplier (Hamamatsu R928) equipped with a liquid He cryostat (Oxford CF1204).

Results and Discussion

Temperature Dependence of the Emission Spectra. The red form of $[Pt(CN)_2(bpy)]$ emits intense luminescence even at room temperature. As shown in Figure 1, the emission spectrum changes remarkably depending on temperature: with decreasing temperature, the spectrum shifts to longer wavelength as well as increasing intensity and sharpening bandwidth. At 15 K, the vibronic structure appears, clearly indicating the MLCT (Pt-(dσ*)→bpy(π*)) character. These spectra correspond to the $E \perp a$ emission reported by Biedermann et al.,[5] and the spectral features are very similar to those for the red form of $[PtCl_2(bpy)]$.[12]

Figure 2 shows the emission spectra of the red form of $[Pt(CN)_2(i\text{-biq})]$ at various temperatures. At room temperature, the emission spectrum is similar to that of $[Pt(CN)_2(bpy)]$. The temperature dependence of the emission spectrum of $[Pt(CN)_2(i\text{-biq})]$, however, is much more complicated: with lowering temperature, sharp peaks appear in addition to the broad one. We have assigned these emission bands at 77 K from multicomponent analysis of the emission decay at several wavelengths before:[8] the emission component with sharp peaks at 569 and 596 nm are due to the $^3\pi\pi^*$(*i*-biq) emission while the broad peak at around 630 nm corresponds to the ^{3}MLCT* emission band. The striking red-shift of the ^{3}MLCT* emission band is not seen for this complex. Though the emission intensity

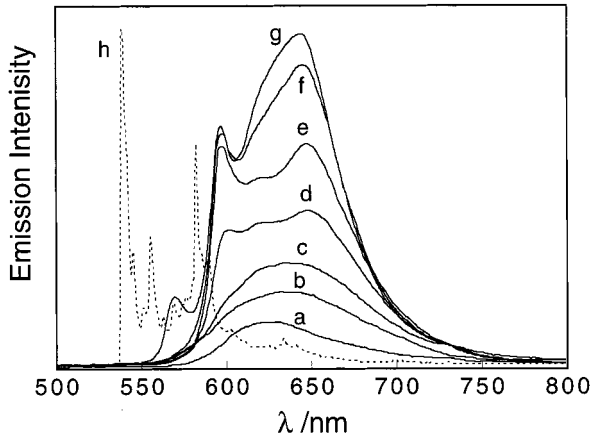

Figure 2. Emission spectra of $[Pt(CN)_2(i\text{-biq})]\cdot 0.5H_2O$ at different temperatures: (a) 293, (b) 200, (c) 177, (d) 150, (e) 125, (f) 100, (g) 77, (h) 2 K. λ_{ex} = 420 nm.

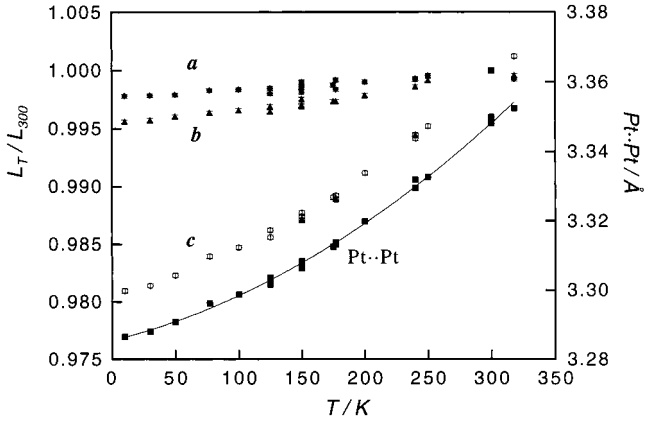

Figure 3. Ratio of cell length (*a*, *b*, and *c*) relative to that at room temperature (300 K) and the Pt···Pt distance for the red form of $[Pt(CN)_2(bpy)]$ plotted as a function of temperature.

increases with lowering temperature, the relative intensity of the ^{3}MLCT* band to the $^3\pi\pi^*$ bands decreases. At 2 K, the ^{3}MLCT* band completely disappeared, and the well-resolved $^3\pi\pi^*$(*i*-biq) emission spectrum was only observed. The 0−0 energy of the $^3\pi\pi^*$ transition (18 620 cm^{-1}) and the features of the vibronic bands are very similar to those for $[Ru(i\text{-biq})_3]^{2+}$, which is known as a rare (α-diimine)ruthenium(II) complex with the $^3\pi\pi^*$ emission state.[13] The ^{3}MLCT* emission of the crystal recovered with increasing temperature.

Temperature Dependence of the Crystal Structures. The accurate crystal structure of the red form of $[Pt(CN)_2(bpy)]$ was recently redetermined by Connick et al.,[3] which contains a staggered (antiparallel) stack of the platinum complexes. We have obtained the same structure at room temperature and found the anisotropic change of the lattice by the variable-temperature measurements (300−15 K) of X-ray diffraction crystallography. The molecular structure was essentially unchanged at lower temperatures. Figure 3 shows temperature dependence of cell lengths represented as the ratio to those at room temperature, and that of the Pt···Pt distance. With decreasing temperature, the *c* axis corresponding to the Pt···Pt stacking direction is particularly contracted compared with the other axes (*a* and *b*). In proportion to the shrink of the *c* axis, the Pt···Pt distance contracts from 3.35 Å at room temperature to 3.29 Å at 15 K.

(11) Crystal Structure Analysis Package, Molecular Structure Corporation: Woodlands, TX, 1985, 1992.
(12) Miskowski, V. M.; Houlding, V. H.; Che, C.-M.; Wang, Y. *Inorg. Chem.* **1993**, *32*, 2518−2524.
(13) Kato, M.; Sasano, K.; Kimura, M.; Yamauchi, S. *Chem. Lett.* **1992**, 1887−1890.

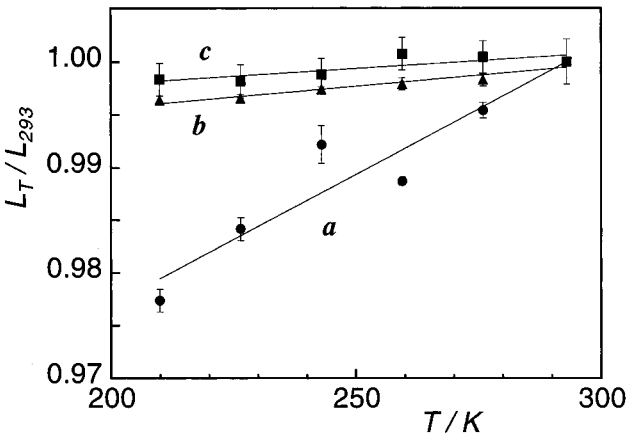

Figure 4. Ratio of cell length (*a*, *b*, and *c*) relative to that at room temperature (293 K) for $[Pt(CN)_2(i\text{-biq})]\cdot 0.5H_2O$ plotted as a function of temperature.

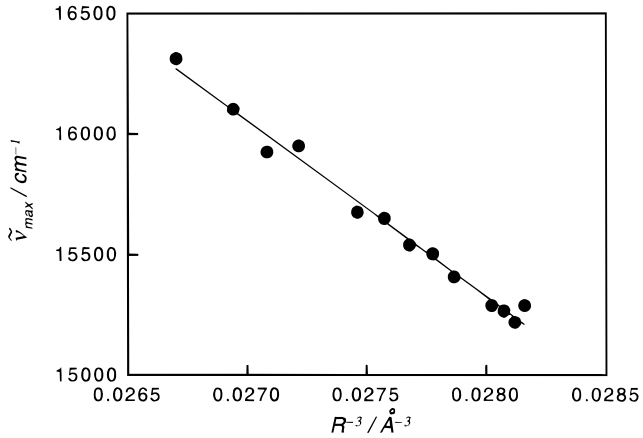

Figure 5. Plot of emission peak energy vs R^{-3} for the red form of $[Pt(CN)_2(bpy)]$, where R is the Pt···Pt distance.

The behavior is very similar to that of the red form of $[PtCl_2(bpy)]$[7] which has the same stacking structure. However, the result of the $[Pt(CN)_2(bpy)]$ stack is noteworthy because the Pt···Pt distance of the $[Pt(CN)_2(bpy)]$ stack is essentially much shorter than those of the $[PtCl_2(bpy)]$ stack (3.45 Å at 300 K to 3.37 Å at 10 K).

In contrast to $[Pt(CN)_2(bpy)]$, the X-ray diffraction measurement of the $[Pt(CN)_2(i\text{-biq})]$ crystal at low temperatures resulted in the specific contraction of the *a* axis (Figure 4), although the fragility of the crystal to the temperature restricted the temperature range measured. The contracted axis does not correspond to the Pt···Pt stacking direction but is normal to the stack (Figure S2). The $[Pt(CN)_2(i\text{-biq})]$ complex is almost planar, and the molecular planes are slightly tilted from the horizontal plane (i.e. (0 0 1) plane) perpendicular to the stacking axis to make a herringbone stacking pattern. The anisotropic contraction of the *a* axis is explained in terms of the change of the inclination of the molecular plane in the stack.

Correlation between the Pt···Pt Distance and the Emission Energy for $[Pt(CN)_2(bpy)]$. Clearly, there is a correlation that the emission spectrum shifts to lower energy with shorter Pt···Pt distance. It is interpreted in terms of the rise of HOMO, the $d\sigma^*$(Pt) orbital derived from the filled d_z^2(Pt) orbital of the monomer complex, with stronger Pt···Pt electronic interaction.[14] As an indicator showing the change of the transition energy of the $[Pt(CN)_4]^{2-}$ chain by the Pt···Pt interaction, a linear relationship between the emission maxima and R^{-3} has been found, where R denotes the Pt···Pt distance in the stack.[6,15] The relationship was well applied to the red form of $[PtCl_2(bpy)]$ although the emission state (^{3}MLCT($d\sigma\rightarrow\pi^*$(bpy)) is different from that for the $[Pt(CN)_4]^{2-}$ chain ($d\sigma^*\rightarrow p\sigma$).[7] We have obtained a good result also for the $[Pt(CN)_2(bpy)]$ system as shown in Figure 5. The data were fitted linearly to give eq 1,

$$\tilde{\nu}_{max}\ (cm^{-1}) = (35.7(7) \times 10^3) - (7.3(3) \times 10^5)R^{-3} \quad (1)$$

The value of $35.7(7) \times 10^3$ cm^{-1} at $R^{-3} = 0$ (i.e., R$\rightarrow\infty$) in eq 1, which means the transition energy for the monomer complex, seems acceptable compared with those for $[PtCl_2(bpy)]$ ($29.5(55) \times 10^3$ cm^{-1})[7] and for $[Pt(CN)_4]^{2-}$ (36 800 cm^{-1}, $E\perp c$; 42 900 cm^{-1}, $E\|c$)[6] because the CN^- ligands with stronger ligand field stabilize the d_z^2 orbital of the square-planar complex much more than that of $[PtCl_2(bpy)]$ containing weak Cl^- ligands.[16] The larger slope of the eq 1 compared with that for the $[PtCl_2(bpy)]$ crystal indicates the higher sensitivity of $\tilde{\nu}_{max}$ against the Pt···Pt distance. It is reasonable in terms of the shorter Pt···Pt distance of the $[Pt(CN)_2(bpy)]$ crystal. Thus the electronic character of the $[Pt(CN)_2(bpy)]$ crystal has been clarified by the correlation between the Pt···Pt distance and the emission energy although the apparent spectral features containing emission energy and the shift resemble that of $[PtCl_2(bpy)]$.

$\pi-\pi$/Pt···Pt Competitive System for $[Pt(CN)_2(i\text{-biq})]$. In the case of the red form of the $[Pt(CN)_2(i\text{-biq})]$ crystal, a blue-shift in emission was apparently observed with decreasing temperature contrary to the red-shift for the $[Pt(CN)_2(bpy)]$ crystal. The unique emission behavior would be due to the multiple emission sites in the crystal. There are some reports on the emission from multiple sites in the solid state of platinum complexes.[17,18] However, the $[Pt(CN)_2(i\text{-biq})]$ crystal is noteworthy because the emission sites have different origins, ^{3}MLCT and $^3\pi\pi^*$(*i*-biq) states. It is due to the fact that the $^3\pi\pi^*$ state of the extended π-system and the ^{3}MLCT state generated by the Pt···Pt interaction happen to come close energetically. For this complex, no distinct red shift of the ^{3}MLCT emission band occurred at low temperature. Consistently with this result, there is no essential change on the Pt···Pt distance between 293 K (3.341(5) Å) and 220 K (3.30(3) Å). Instead, the inclination of the $[Pt(CN)_2(i\text{-biq})]$ plane in the stack varied with temperature (5.1° at 293 K, 10.5° at 220 K). The characteristic change of the crystal structure of $[Pt(CN)_2(i\text{-biq})]$ would be attributed to the effect of the $\pi-\pi$ interactions between the *i*-biq ligands both in and out of the stack. Simple thermal shrinkage of the Pt···Pt distance may be prevented by the van der Waals repulsion between π orbitals of the ligands in this case. Thus the $\pi-\pi$ and Pt···Pt interactions of the system work competitively to realize unusual changes of the structure and the emission behavior.

Acknowledgment. This work was supported by a Grant-in-Aid for Scientific Research (Nos. 08640712, 09640667, and 10149234) from the Ministry of Education, Science, Sports and Culture.

(14) Thomas, T. W.; Underhill, A. E. *Chem. Soc. Rev.* **1972**, *1*, 99.
(15) Day, P. *J. Am. Chem. Soc.* **1975**, *97*, 1588−1589.
(16) The energy of the ^{3}MLCT state for the monomer complex of $[Pt(CN)_2(bpy)]$ cannot be detected directly by spectroscopy because the emission state (*i.e.* the lowest excited state) is not ^{3}MLCT but $^3\pi\pi^*$ ($\tilde{\nu}_{max} = 22.2 \times 10^3$ cm^{-1}).
(17) Büchner, R.; Field, J. S.; Haines, R. J.; Cunningham, C. T.; McMillin, D. R. *Inorg. Chem.* **1997**, *36*, 3952−3956.
(18) Miskowski, V. M.; Houlding, V. H. *Inorg. Chem.* **1989**, *28*, 1529−1533.

Supporting Information Available: Figures of the molecular structure at 293 K, the crystal packing at 293 and 220 K for $[Pt(CN)_2(i\text{-biq})]\cdot H_2O$, a packing diagram at 293 K for $[Pt(CN)_2(bpy)]$, and a table of lattice parameters for $[Pt(CN)_2(bpy)]$ at 10−318 K. X-ray crystallographic files, in CIF format, for $[Pt(CN)_2(bpy)]$ at 293K and $[Pt(CN)_2(i\text{-biq})]\cdot 0.5H_2O$ at 293 and 220 K are available. This material is available free of charge via the Internet at http://pubs.acs.org.

IC981027A